J Radioanal Nucl Chem (2016) 309:1133–1143
DOI 10.1007/s10967-016-4714-8

Sediment geochronology and geochemical behavior of major and rare earth elements in the Oualidia Lagoon in the western Morocco

N. Mejjad[1] · A. Laissaoui[2] · O. El-Hammoumi[1] · M. Benmansour[2] · S. Benbrahim[3] · H. Bounouira[2] · A. Benkdad[2] · F. Z. Bouthir[3] · A. Fekri[1] · M. Bounakhla[2]

Received: 24 October 2015 / Published online: 29 January 2016

Abstract Naturally occurring radionuclides and ^{137}Cs were measured in a sediment core and surface deposit collected from the bed channel of the Oualidia Lagoon located in the western Morocco. Major and rare earth elements (REE) profiles were determined by instrumental NAA technique. ^{210}Pb and ^{137}Cs were used to establish the sedimentation chronology over the last decades by using conventional models. ^{210}Pb displayed relatively higher concentrations and rate of supply to the sediment than typical levels found in other coastal areas in Morocco. REE ratios and Ce anomalies showed that the direct incorporation of particles from seawater to the bed sediment is the most important, followed by the terrigenous component.

Keywords The Oualidia lagoon · Marine geochemistry · ^{210}Pb radiometric dating · Neutron activation analysis · Rare earth elements

Introduction

Sediments are considered as one of the most important archives of radiological and geochemical data which, in combination with radiometric dating, provide prominent information regarding the ecological processes occurring in coastal ecosystems. The Oualidia lagoon is a coastal aquatic environment located in the western Moroccan Atlantic Ocean coast. It is about a shallow inland body of seawater of about 7 km length parallel to the coastline, separated from the ocean by a sand barrier. It is connected to the Atlantic Ocean by one permanent inlet of 150 m width and a small secondary inlet active in spring tides. The water in the Lagoon is mainly seawater since it is about a lagoon without a river and the only freshwater inputs come from rainfall over the region, which constitute a small contribution during rainy seasons to the overall water budget in the Lagoon [1]. Water currents are generally weak; the strongest currents during spring tides are about 1.25 $m.s^{-1}$ registered near the entrance of the lagoon in the south, and decrease northward reaching values as low as 0.35 $m.s^{-1}$. On the other hand, currents during neap tides are extremely weak, not exceeding 0.2 $m\ s^{-1}$ [2]. The bed channel exhibit a variety of sediment types with a predominance of sandy sediment in the centre of the main channel, while in most marginal areas sediments contain relatively high percentages of mud (silt/clay).

Although several environmental studies have been carried out in the Oualidia Lagoon with the aim to assess its state of pollution and functioning [3, 4], characterization and geochemistry of major elements (ME) and rare earth elements (REE) in such important ecosystem has received relatively minor attention. These elements have been widely used worldwide as tracers of biogeochemical and weathering processes in marine aquatic systems [5–7]. Indeed, REE in sediment could reflect the influence of several parameters related to both marine water geochemistry and terrigenous inputs, since they have similar chemical properties so that they are less affected by fractionations during the post-depositional processes [8]. On

✉ A. Laissaoui
laissaoui@cnesten.org.ma

[1] Laboratoire de Géologie Appliquée, Géomatique et Environnement - Faculté des Sciences - Ben Msik, Casablanca, Morocco

[2] Centre National de l'Energie, des Sciences et Techniques Nucléaires – Rabat, Rabat, Morocco

[3] Institut National de Recherche Halieutique, Casablanca, Morocco

the other hand, radiometric dating using ^{210}Pb and ^{137}Cs as chronometers provides the age-depth relationship for sediment deposited over the last century. Such information is helpful in interpreting element profiles in the sediment and reconstruction of the history of the depositional environment [9]. A review of potentials and limitations of sediment dating models using ^{210}Pb as a chronometer can be seen in Kirchner [10]. ^{40}K is usually used as a proxy for sediment composition, mainly clay content and biogenic sedimentation.

The main objectives of this study are the following:

(i) to assess the activity distribution of radionuclides (^{210}Pb, ^{137}Cs, ^{226}Ra, ^{40}K) in a sediment core collected from the Oualidia lagoon, and the use of excess ^{210}Pb profile to establish the relation age-depth in sediment, accumulation rates, inventory and rate of delivery. Variations of radionuclide concentrations with grain size are also studied.

(ii) to provide a data-set on ME and REE distribution along the core and to use some selected elements as proxies to establish the origin of the deposited sediment and their geochemical behavior.

(iii) to investigate REE incorporation to the depositional environment and their fractionation through elemental ratios and Cerium anomalies.

Materials and methods

Sampling and sample pre-treatment

A sediment core of 26 cm was retrieved at low tide (the water depth was about 1 m) from the main channel belonging to the Oualidia lagoon in September 2012 using an Uwitec gravity corer of 10 cm internal diameter. Surface sediment (6 cm thickness) was also collected at low tide from a marginal area adjacent to the coring site. The sampling location (Fig. 1) lies in the main channel, and was selected on the basis of hydrodynamic conditions considerations [2]; the maximal water depth is <2.0 m and tidal currents are predominantly weak (<0.40 m/s), which may promote the settling of sediment particles. Furthermore, the sampling site belongs to the intermediate zone of the lagoon where both marine and continental influences prevail [11].

The sediment core was sectioned into 1–2 cm slices, using a core cutter provided with a cutting foil of 0.5 mm, ejection piston and distance holder with distance blades of 0.5 cm each one. This operation was carried out immediately after retrieval to avoid particles redistribution, and then transported to the laboratory for pre-treatment and conditioning prior to radiometric and elemental analyses.

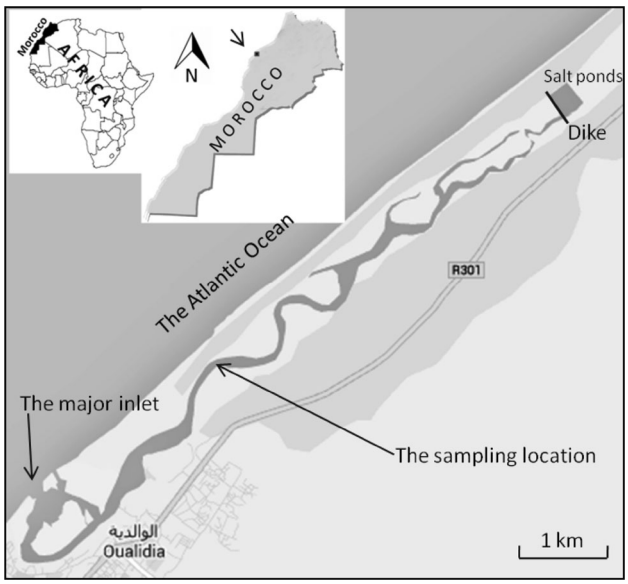

Fig. 1 Map of the Oualidia Lagoon showing the location of the sampling point

Each one of the resulting sub-samples along with the surface sample were dried in an oven at a constant temperature of 80 °C during 24 h. Bulk densities were determined from weight and volume calculations. Finally, dried sediment was mechanically disaggregated (this is a delicate process, since we tried to preserve the naturally occurring particles) for subsequent grain size distribution determination and separation. Particle size distributions were determined in the homogenized sub-samples using a wet Laser Diffraction equipment (Malvern Mastersizer 2000) using the Hydro 2000G dispersion Unit. The particle size distribution range is 0.02–2000 μm. A small amount of sample (~1 g) was introduced in the dispersion unit containing demineralised water, used as dispersant, and then measured after a brief time (10 s) of ultrasound application to disperse any agglomerates. Reproducibility of measurements was assessed by analysing each sample in duplicate, and the results were acceptable, reflecting the homogeneity of the samples. On the other hand, The dried surface sediment was sieved for 6 h in a sieving pile mounted on a vibration shaker to separate the different grain size fractions. Organic matter content was calculated as the difference in weight between the dried sediment and the ash obtained following ignition at 550 °C for 24 h.

Radionuclide determination

Activity of ^{210}Po was determined more than a year after sampling, so it was assumed that secular equilibrium with its parent ^{210}Pb in the topmost layers had been achieved. An aliquot of about 0.5 g of dry sediment was weighed in an acid cleaned beaker, spiked with a known activity of

^{209}Po yield tracer (the certified specific activity is 0.357 ± 0.011 Bq g^{-1}) and totally digested using concentrated nitric and perchloric acids. A review of ^{210}Po determination can be seen in Mathews et al. [12]. The digested sample was evaporated to almost dryness and treated by evaporation with concentrated hydrochloric acid three times and, finally, dissolved in 80 ml of 0.5 N HCl. About 50 mg of ascorbic acid was added to reduce any iron present in the solution. Polonium was auto-deposited onto a Platinum coated disc for 6 h of heating at 80 °C and stirring of the solution. The prepared alpha-sources were analysed by alpha-ray spectrometry using silicon surface barrier detectors (EG&G) coupled to a PC running Maestro™ data acquisition software. The chemical recovery values ranged from 60 to 90 %. Excess ^{210}Pb concentrations were determined by subtracting the depth averaged concentration of ^{226}Ra, supposed to be in secular equilibrium with supported ^{210}Pb, from total lead-210 [13].

Gamma emitting radionuclides (^{228}Ac(^{228}Ra), ^{214}Bi(^{226}Ra), ^{234}Th, ^{40}K and ^{137}Cs) were measured by high resolution gamma-ray spectrometry. The detector used was a low background CANBERRA hyper-purity germanium p-type coaxial detector, housed in a 10-cm-thick high-purity lead shield. The relative efficiency was 30 % and the resolution was 2 keV for the 1332 keV ^{60}Co γ-peak. Weighed samples were introduced into 20 ml nalgene containers and sealed to trap the gaseous ^{222}Rn and ^{220}Rn emanating from in situ ^{226}Ra and ^{224}Ra, respectively. The flasks were stored for more than 21 days and then counted for 24 h each one. In some cases, and due to the small quantities of sediment in the upper layers of the core, we combined two adjacent sub-samples to reach the working geometry. ^{226}Ra was obtained from ^{214}Bi photopeak at 609.3 keV, ^{228}Ra from ^{228}Ac at 911 keV, while ^{234}Th was determined from the photopeak 63 keV after correction for self-absorption. The correction factor was determined by measuring an ^{241}Am point source placed over the container filled with sediment and the empty container, as in the procedure used by Ramos-Lerate et al. [14].

Energy and efficiency calibrations of the gamma spectrometer were carried out using a multigamma standard solution provided by Amersham in the same geometry as the samples. Correction due to coincidence summing effect, in the case of ^{214}Bi determination, was carried out by measuring the reference material IAEA-326 in the same geometry. The activity concentration (in Bq kg^{-1}) in each sample of all the studied radionuclides was determined from the net count rate under the photopeak of interest, detector efficiency, gamma intensity and sample weight. The analytical procedure was checked using reference material (IAEA-327). The relative difference between measured and certified values was less than 10 % for all radionuclides present in the reference material.

Metal determination by neutron activation analysis

Irradiations of sediment samples were carried out at neutron activation analysis laboratory in the National Centre for Energy, Sciences and Nuclear Techniques (CNESTEN) hosting the first Moroccan Triga Mark II research reactor which provides mainly thermal neutrons, with a flux of 5.0 10^{12} n cm^{-2} s^{-1} at the pneumatic transfer system (PTS) and 2.0 10^{13} n cm^{-2} s^{-1} at the rotary specimen rack. Neutron activation analysis technique was used for the determination of major and rare earth elements. Thus, two types of irradiation have been performed according to the period of the elements to be measured (irradiations of 30–60 s for the elements with short periods and of 4 h for elements with long periods). For short irradiations; each sample was prepared with flux monitor (approximately 500 mg of powder sublimed sulfur). Both sample and flux monitor are then locked in a polyethylene rabbit. These were transferred to the reactor core via a pneumatic transfer system which allows irradiation sample by sample.

In the case of long irradiations, about 200 mg of each sample were sealed into a pure polyethylene container. They were placed in a polyethylene rabbit with 5–10 mg of cobalt wire (Al/Co alloy containing certified 1 % Co), used as a neutron flux monitor, and 200 mg sample of the standard reference material (NIST 2711—Montana Soil) prepared and irradiated similarly. The prepared rabbits were then transferred to the "rotary specimen rack" system containing 40 irradiation positions. In order to take into account the flux variation in this system, two flux monitors (Cobalt wire) were placed in a separate rabbit.

Counting of emitted gamma rays was performed using a hyper-purity germanium detector (HPGe). Data acquisition was performed using Maestro software and calculations of concentrations were made by the K0_IAEA software.

The Standard Reference Material was used for the determination of elemental concentration, intercomparison purposes, and also to assess the precision of the technique used. The values found were in acceptable agreement with the certified values, and also the reproducibility of the INAA. The precision was found to be better than 10 % for most of the elements. The performance for accuracy was assessed by *Z*-scores, which were calculated for each element. Results obtained for all elements are generally well clustered around the reference value ($|Z| < 3$).

Particle size measurements

In conjunction with radionuclides and metals analyses, grain size composition throughout the sediment core was determined and the corresponding profile is shown in Fig. 2. The sediment core is mainly sand with predominance of medium sand ($250 < D < 500$ μm), and some

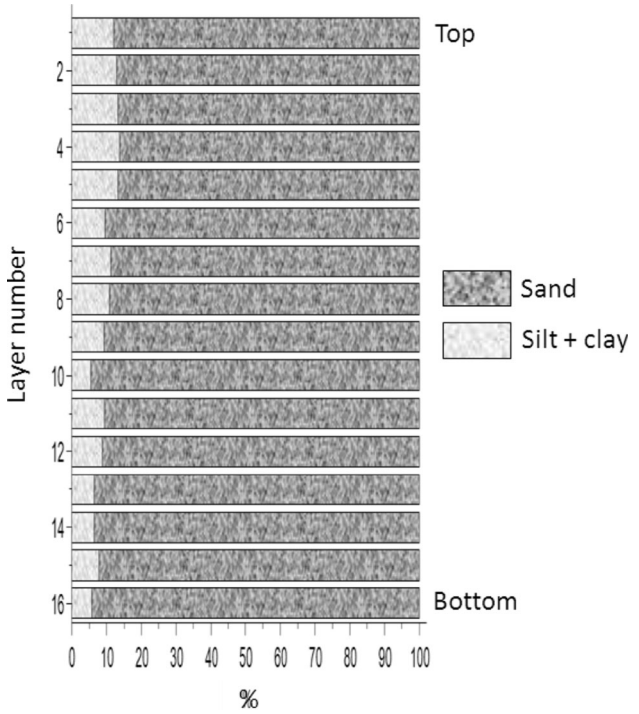

Fig. 2 Grain size distribution in the sediment core collected from the bed channel

variations of mud (silt/clay) content throughout the core were observed. The percentages of mud were ranging from 6 to 13 %. On the other hand, the surface sediment collected from a marginal area adjacent to the core sampling point was composed of nearly 30 % of mud and 70 % of sand.

Results and discussion

Radionuclides in grain size fractions of surface sediment

Gamma emitting radionuclides (^{210}Pb, ^{137}Cs, ^{234}Th, ^{226}Ra, ^{228}Ra and ^{40}K) were measured in the bulk surface sediment as well as in different grain size fractions. The corresponding profiles are shown in Fig. 3. Levels of ^{226}Ra, ^{228}Ra, ^{234}Th (in equilibrium with ^{238}U) and ^{40}K were of the same order of magnitude of those recorded in sediments from non-contaminated aquatic environments. It has been observed an important range of variation in radionuclide concentrations with particle size distribution; all the studied radionuclides are present in highest concentrations in the fine fractions (diameter <50), followed by the sand-sized particles of diameters greater than 710μm. Indeed, values in the mud-sized particles are larger, of more than twice, than those in average diameters between 88 and 250 μm, and around 1.66 times in the coarsest fraction >710 μm, except for ^{210}Pb which presented a ratio of only 1.33. This is in good agreement with earlier experimental studies such as the work published by He and Walling [15] who reported that ^{137}Cs and ^{210}Pb are primarily adsorbed by finer particles and their concentrations associated with coarse particles increase with increasing sand content in the sample. Activities of ^{226}Ra were ranging between 15 and 40 Bq kg^{-1}, so that ^{210}Pb present in the studied surface sediment, whose concentrations in each size fraction was one order of magnitude higher than those of ^{226}Ra, is unsupported. About 50 % of ^{210}Pb and ^{137}Cs concentrations in the bulk sediment was found in the <75 μm average diameter fraction, and 15 % in the coarse fraction between 0.72 mm and 1.355 mm. It is well known from previous studies that fine particles play an important role in adsorption and scavenging of particle reactive radionuclides in natural aquatic systems [16]. Obviously, small sized particles have a greater specific surface area and therefore a larger capacity to adsorb dissolved radionuclides and metals, which result in enhanced concentrations in fine particles. The presence of radionuclides in important amount in the sand fraction greater than 710 μm is well correlated with the high amount of organic matter (∼4 %) compared to the other fractions. It was well established that organic matter coatings onto mineral particles increase the adsorption capacity of dissolved radionuclides [16].

Radionuclides in the sediment core

^{40}K and ^{228}Ra concentration profiles are shown in Fig. 4. The values found for these naturally occurring radionuclides were of the same ranges of typical concentrations recorded in coastal environments (100–700 Bq kg^{-1}for ^{40}K and 10–50 Bq kg^{-1} for ^{228}Ra) [17]. The profiles showed fluctuations with discrete minima and/or maxima throughout the core (100–400 Bq kg^{-1} for ^{40}K and 10–40 Bq kg^{-1} for ^{228}Ra). Concentrations of ^{40}K ranging from 300 to 550 Bq kg^{-1} were found in a sediment profile from the Sebou Estuary, also lying on the Atlantic Ocean. On the other hand, ^{226}Ra concentration was fairly uniform along the core with a mean value of 30.28 Bq kg^{-1}.

Figure 5 depicts the vertical distribution of excess ^{210}Pb. Mass depth (in g cm^{-2}) was used instead of depth (in cm) to account for sediment compaction [18]. Concentration levels of this radionuclide are much lower than those reported in an earlier study carried out in the same site [3, 4], and much higher than the concentrations found in sediments from the Sebou Estuary [19]. Low Pb-210 concentrations are due to the low percentages of fine-sized particles (silt and clay) which were ranging between 6 and 13 % in all sections of the core as showed in Fig. 2. Nevertheless, the relatively high content of coarse sediment

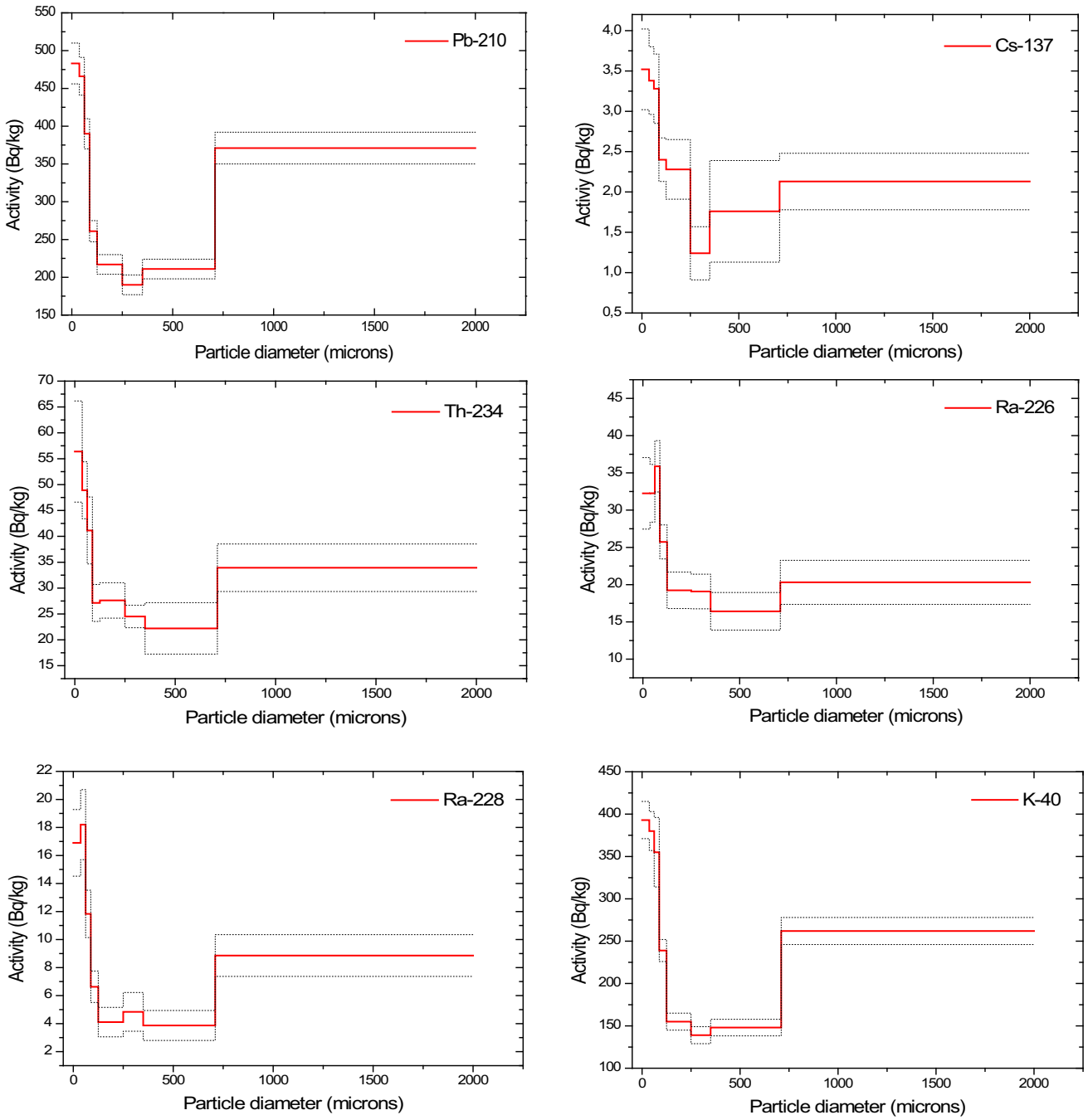

Fig. 3 Radionuclide concentrations versus particle diameter. The *dotted lines* are $1-\sigma$ statistical error range

having relatively lower affinity for dissolved radionuclides did not restrict dating of our sediment core.

The excess ^{210}Pb profile of Fig. 5 exhibit an exponential decay of activities with depth, but was qualified as being incomplete, since concentrations did not decline to zero in the deepest layers. Consequently, the core cannot be dated by the Constant Rate of Supply model, but the application of the conventional simple model CF-CS (Constant Flux—Constant Sedimentation) could be appropriate in this case. This ultimate supposes that the amount of ^{210}Pb delivered to the sediment and sedimentation rate are constant over a time comparable to the age of the core, and excludes any post-depositional mixing and/or diffusion. Thus, the ^{210}Pb specific activity should display an exponential decay similar to the curve shown in Fig. 5. The line is the best fitting to a first order exponential expression in the form $P_1.\exp(-P_2.x)$, where P_1 is the concentration at the sediment–water interface and P_2 the ratio λ/v_s (λ is the ^{210}Pb

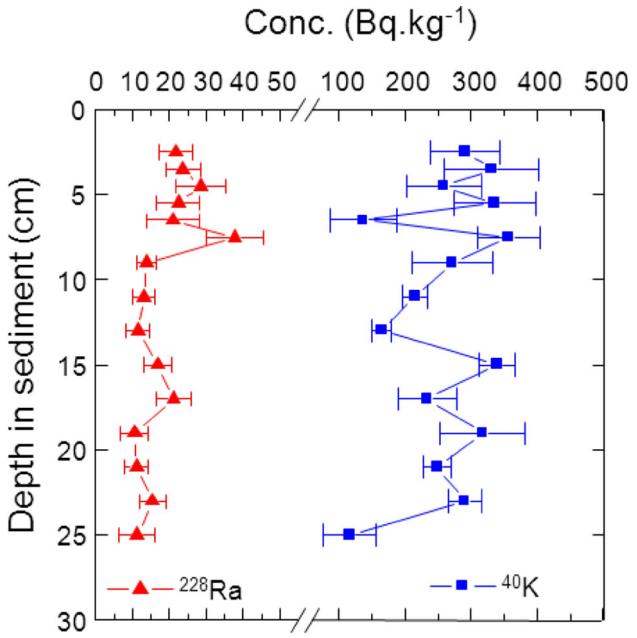

Fig. 4 ^{40}K and ^{228}Ra concentrations in the sediment core from the Oualidia Lagoon. *Errors* are $1-\sigma$ statistical uncertainties

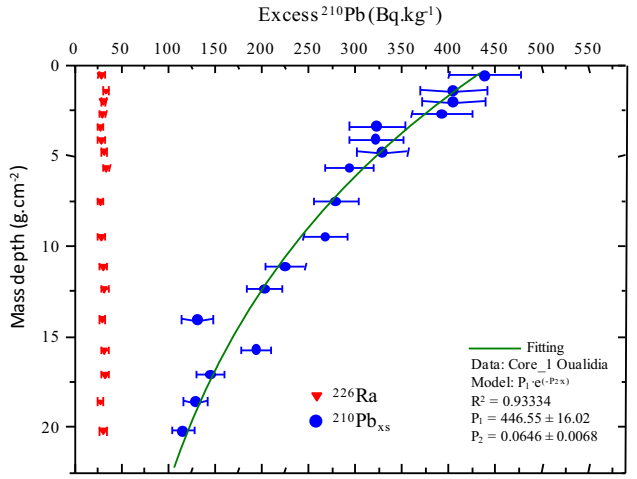

Fig. 5 Vertical profiles of ^{226}Ra and excess ^{210}Pb concentration, in Bq kg^{-1} dry weight, in the sediment core from the Oualidia Lagoon. The *points* are the experimental data, with their $1-\sigma$ error, and the line is the best fit to a first order exponential decay function

decay constant and v_s the accumulation rate). The CF-CS model provided an average accumulation rate $v_s = 0.48 \pm 0.05$ g cm^{-2} y^{-1}, and the ^{210}Pb rate of supply to the sediment ($F = A(0).v_s$ being $A(0)$ the activity of the topmost layer) was $F = 2148 \pm 238$ Bq m^{-2} y^{-1}.

It is worth noting that the calculated excess ^{210}Pb supply rate is substantially higher than those established in other coastal environments and also in the Mediterranean Basin (the annual rate of supply was 720 Bq m^{-2} y^{-1}). Two reasons could be behind this ^{210}Pb enhancement in the sediment: (1) an excessive presence of the gaseous ^{222}Rn in the atmosphere of the studied region most probably due to anthropogenic activities, and (2) the upwellings prevailing in the Moroccan Atlantic coast [20, 21] which produce the rising of deep oceanic waters rich enough of ^{210}Pb resulting in higher inventories in the lagoon sediment. Indeed, relatively high inventories were attributed in other environments to the upwelling activity such as in the south Pacific Mexico [22].

^{210}Pb chronology should be confirmed by a second independent tracer. ^{137}Cs, which is an artificial radionuclide resulting from nuclear bomb testing and detonations since early 1945, can be used as a horizon marker to identify the period of maximum atmospheric fallout. The vertical distribution of ^{137}Cs concentrations along the core is plotted in Fig. 6. Concentrations ranged between 1.5 and 3.9 Bq kg^{-1}, being similar to those reported in the literature for coastal environments [9] but apparently lower than those reported in a recent study in the same region (5–13 Bq kg^{-1}) [4]. These relatively small concentrations are likely to be attributed to the low content of fine-grained particles which have high adsorption capacity of radionuclides than sandy sediment. Concentrations in the upmost layers were below the limit of detection due to the low amount of samples. Unfortunately and due to the reduced length of our core, the profile did not reveal any defined peak that can be used as time marker. However, ^{137}Cs concentrations presented a growth trend in deep layers below 17 cm reaching the maximum value at the deepest section of the core. According to CF-CS ages, the basal layer corresponds to the year 1972 ± 4 so that the peak of maximum global fallout of 1963 should be below this layer.

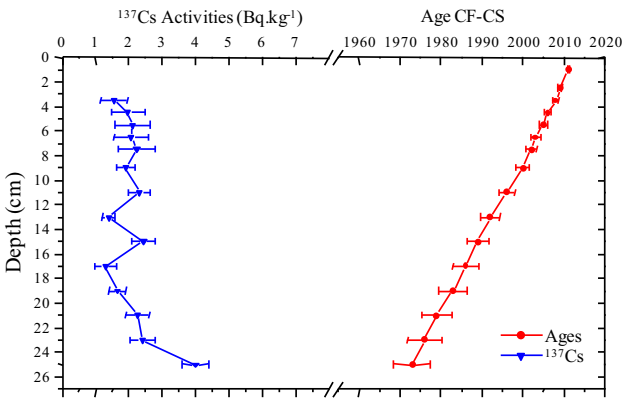

Fig. 6 Profiles of calculated ages using the CF-CS model, and distribution of ^{137}Cs concentrations versus depth. The *values* for upmost layers were below the limit of detection due to the low amount of samples (high water content)

Input of major and rare earth elements to the sediment

Major elements

Concentrations of rare earth and major elements were measured in the sediment core collected from Oualidia Lagoon by using the Instrumental Neutron Activation Analysis (IAAN). Concentration profiles of 8 major elements are plotted in Fig. 7 along with the approximate layers' ages provided by ^{210}Pb chronology presented in the previous section. In general, major elements distributions in sediment displayed some variability with discrete minima and maxima throughout the core. The highest values for almost all elements were recorded in a deep layer (21 cm) corresponding to the period around 1980.

Al, Ti, Mn and Fe profiles presented moderate variations along the core (1.69–5.20 %; 0.11–0.31 %, 75–302 μg/g and 0.91– 1.65 %, respectively). Concentrations of the three elements, Al, Mn and Fe, were lower than the mean crustal abundances (8.2 % for Al, 950 μg/g for Mn and 5.6 % for Fe; [23]), while Ti was present in much higher concentrations than the mean crustal abundance (0.57 mg/g), being all within the range of values reported for sediments from Bouregreg river [24]. As these elements are used as indicators for input of terrigenous materials to the sediment, their variation should reflect the contribution of weathered sediment from the continental surrounding area. Fe and Mn, which are two redox-sensitive elements, did not show similar behaviour along the core. A noticeable increase in Mn content along the sediment core was observed at a depth around 21 cm, while Fe presented fairly uniform distribution along the core. In addition, Fe is not correlated to any other major element (Table 1) with the exception of a weak negative correlation with Ca was observed ($r = -0.632$ at $P < 0.005$, $N = 15$), while, on the contrary, Mn is significantly correlated to all elements, except to Fe. The high correlation between Ca and Mn suggest that Mn is mainly incorporated during calcite precipitation from seawater. This behavioural difference between Fe and Mn is mainly due to changes in the formation and precipitation of Fe and Mn oxyhydorxides, and also to their different degree of redissolution in prevailing redox conditions in sediment depth [25]. Al/Ti ratio is a good indicator of terrigenous input to the sediment [6]. The study area is surrounded by sandy dunes, so that the most likely mode of transport of particles must be aeolian and runoff following heavy rain episodes.

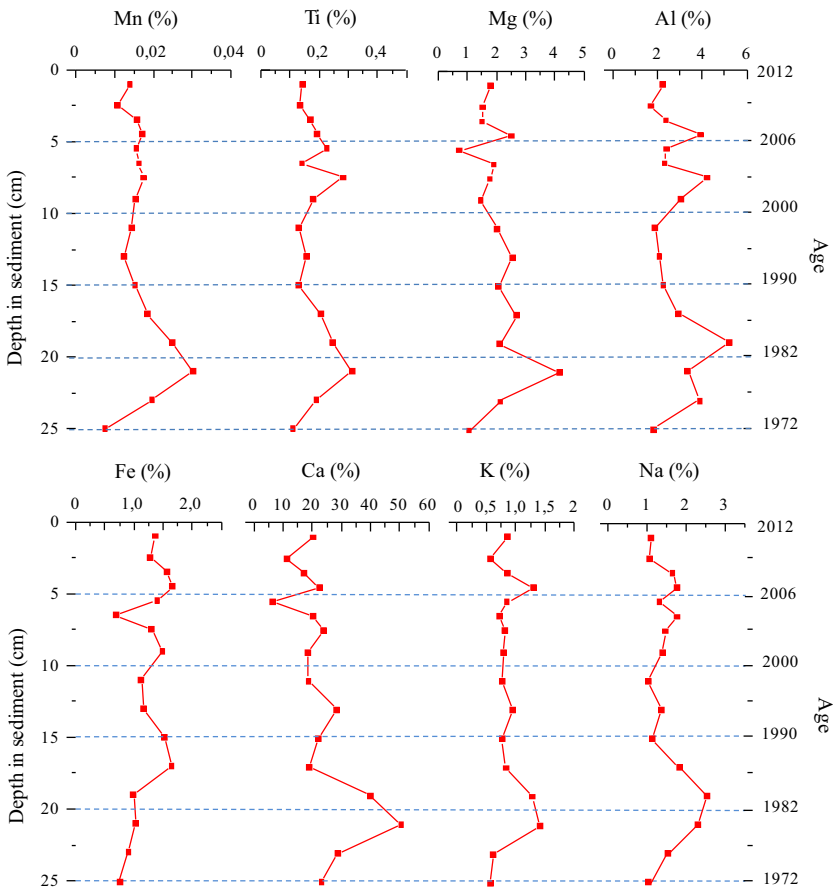

Fig. 7 Profiles of major elements in the sediment core collected from the Oualidia Lagoon. Approximate layers' ages based on ^{210}Pb chronology are also given

Table 1 Pearson correlation matrix for major elements in the sediment core from ElOualidia Lagoon

	Al	Fe	Ca	Na	K	Mg	Ti	Mn
Al	1.000							
Fe	−0.173	1.000						
Ca	**0.553**	**−0.632**	1.000					
Na	**0.785**	−0.272	**0.773**	1.000				
K	**0.667**	−0.298	**0.835**	**0.828**	1.000			
Mg	0.210	−0.314	**0.780**	**0.567**	**0.717**	1.000		
Ti	**0.756**	−0.336	**0.743**	**0.777**	**0.651**	**0.574**	1.000	
Mn	**0.663**	−0.404	**0.892**	**0.879**	**0.805**	**0.734**	**0.845**	1.000

Bold values indicates the significant correlation at $P < 0.005$

Al/Ti ratios throughout the core exhibit large variations (Table 2) from 10, characteristic of marine sediment, to 21 closer to values for the upper continental crust [26]. The depth averaged value is 15.68, which is indicative of the contribution of continental materials in the bed sediment. In addition, Al profile displayed some peaks of higher concentrations which likely correspond to rainy years, and a relative depletion between 1990 and 2000 during which the longest droughts were registered in Morocco.

On the other hand, K/Al ratios presented a wider range of variation throughout the core, from 0.16 to 0.46 with a mean value about 0.30 being in general higher than that reported for the continental crust (0.22). Although K is one of the major elements in seawater and has a certain affinity to clay minerals, most of potassium in marine sediment is associated with terrestrial materials [27].

Table 2 K/Al, Ca/Mg and Al/Ti ratios throughout the sediment core

Layer	K/Al	Ca/Mg	Al/Ti
1	0.38	11.28	15.87
2	0.34	7.38	12.65
3	0.36	11.33	14.12
4	0.33	8.87	20.54
5	0.35	8.89	10.57
6	0.31	10.60	16.43
7	0.19	13.35	14.95
8	0.26	12.72	16.83
9	0.40	9.19	14.68
10	0.46	11.14	13.49
11	0.34	10.59	17.44
12	0.28	7.03	14.28
13	0.25	18.74	21.20
14	0.42	12.15	10.76
15	0.16	11.36	20.47
16	0.31	21.92	16.70
MIN	0.16	7.03	10.57
MAX	0.46	21.92	21.20
MEAN	0.32	11.66	15.69
St devia	0.08	3.86	3.20

Minimal, maximal, mean and standard deviation values are also given

Ca and Mg presented fairly uniform distribution until the depth of 19 cm after which a visible increase down core peaked at 21 cm for both elements. Ca/Mg ratios were within the large range between 7 and 22 with a mean depth averaged value of 11.66, being much higher than typical values of carbonate rocks and ratios reported for sediment [28].

Rare earth elements

Nine rare earth elements (La, Ce, Nd, Sm, Eu, Dy, Tb, Yb, Lu) were measured in the sections composing the sediment core and the profiles were plotted in Fig. 8. These are to our knowledge the first such data on REE contents in sediment from the Oualidia lagoon. The concentrations were in general higher than those recorded in Bouregreg estuary [24]. Correlation coefficients among individual REE and between REE and major elements are given in Table 3.

In general, the REE profiles showed large variations and displayed maxima and minima throughout the core, without being similar to one another, which reflect the variability of the depositional environment throughout the years. It is well established that REE in coastal sediments have mainly two components: (1) a land-derived source as a result of weathering and aeolian transport processes, and (2) a seawater source as a consequence of precipitation with biogenic carbonate and Fe–Mn oxyhydroxides.

Lanthanum exhibits significant positive correlation with Ce, Tb and Yb, and only with one major element, Fe. Ce showed correlation with Tb and Yb, while Sm and Nd displayed no significant correlation with any REE or major elements. Eu gave positive correlation with Dy and more or less significant correlation with all major elements except Fe and Al. In the case of Dy and Eu, they correlate well with all major elements but not with Fe. Overall strong to moderate relationship of La, Ce, Nd, Tb and Yb with Fe, but not with Mn, indicated the preferential association of these elements with Fe oxyhydroxides. On the other hand,

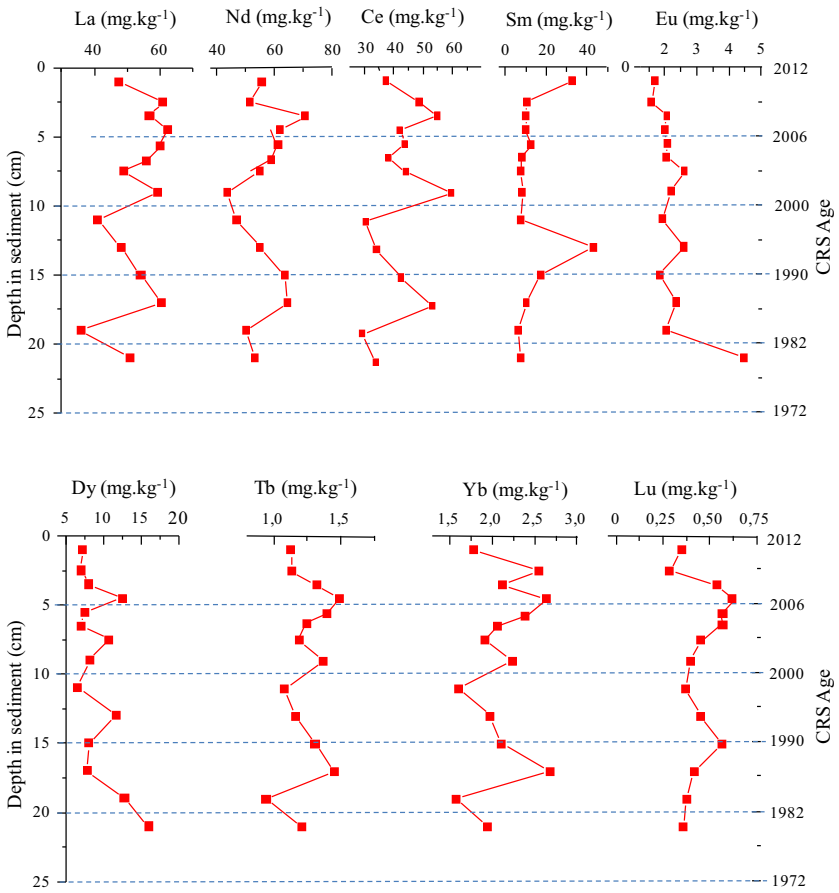

Fig. 8 Profiles of rare earth elements in the sediment core collected from the Oualidia Lagoon. Approximate layers' ages provided by ^{210}Pb chronology are also given

Table 3 Correlation tables REEs/Major elements and REEs/REEs

	Al	Fe	Ca	Na	K	Mg	Ti	Mn	La	Ce	Nd	Sm	Eu	Dy	Tb	Yb	Lu
La	−0.18	**0.83**	−0.40	−0.26	−0.11	−0.09	−0.01	−0.24	1.00								
Ce	−0.16	**0.66**	−0.53	−0.23	−0.43	−0.38	−0.10	−0.32	**0.76**	1.00							
Nd	0.08	**0.67**	0.11	0.04	0.18	0.29	−0.01	0.02	0.45	0.26	1.00						
Sm	−0.39	0.03	0.00	−0.36	−0.08	0.06	−0.38	−0.41	−0.07	−0.24	0.16	1.00					
Eu	0.27	−0.25	**0.74**	**0.53**	**0.60**	**0.77**	**0.74**	**0.76**	−0.03	−0.20	0.03	−0.08	1.00				
Dy	**0.66**	−0.18	**0.86**	**0.71**	**0.90**	**0.73**	**0.73**	**0.76**	−0.08	−0.39	0.19	−0.01	**0.75**	1.00			
Tb	−0.05	**0.78**	−0.28	−0.08	0.04	0.08	0.01	−0.10	**0.82**	**0.69**	0.46	−0.11	0.06	−0.02	1.00		
Yb	−0.11	**0.71**	−0.37	−0.12	−0.09	0.01	−0.06	−0.23	**0.92**	**0.69**	0.42	−0.11	−0.10	−0.07	**0.80**	1.00	
Lu	0.15	**0.52**	−0.15	0.02	0.20	−0.08	−0.04	−0.08	0.32	0.19	0.43	0.01	−0.12	0.10	**0.61**	0.29	1.00

Bold values show correlations are significant at $P < 0.05$

Eu and Dy precipitate rather with Mn and carbonate phases as they are correlated to all major elements, except to Fe, with the exception of the pair Eu–Al.

REE ratios could indicate the origin of particles in the depositional environment. Indeed, $Nd/Yb)_{SN}$ ratio (*SN* is shale normalized) displayed values between 1.70 to 3.80 along the core, all greater than typical ratios proposed for shallow seawater (0.205–0.497) [29, 30] suggesting that the original seawater signal in the lagoon sediment is altered by another source of REEs. In addition, the $Dy/Yb)_{SN}$ ranged from 1.77 to 5.28 along the core, much greater than the values characteristic of seawater. Thus, the enrichment of REE in the bed sediment of the Oualidia Lagoon could be explained by enhanced REE in seawater entering the lagoon and/or the predominance of lithogenic component. Nevertheless, $La/Yb)_{SN}$ ratio indicative of REE

fractionation displayed a depth averaged value of 17.2 with minor scattering along the core, suggesting a relatively high degree of enrichment of light REE with respect to heavy REE. Additionally, its values were all much greater than those recorded for terrigenous particulate matter, 1 and 1.3 [22, 31] implying that the land-derived component of REE in the studied bed sediment is not conserved.

Cerium anomaly is a widely used parameter for establishing the origin of the deposited sediment in coastal systems [32, 33]. Ce anomalies arise from the modification in its valence state (from Ce^{3+} to Ce^{4+}). Ce/Ce* were calculated by using the approach adopted by Minai et al. [34], where Ce* values in each section of the core were estimated using an expression containing the corresponding chondrite-normalized concentrations of Ce, La and Sm. The values obtained were all below 1 (0.58–0.93) reflecting negative anomalies throughout the core. Cerium anomaly is characteristic of oceanic waters; the typical values of Ce/Ce* in seawater were reported to be within the range of <0.1 and 0.4 [35]. The values found in this work indicate that there was a high proportion of REE incorporated directly from seawater through adsorption onto biogenic materials and/or with oxyhydroxide precipitates. However, the lack of correlation between Ce and the redox-sensitive element, Mn, exclude any significant deposition under oxic conditions while, on the contrary, the correlation with iron suggest Ce precipitation with Fe oxides and/or iron bearing minerals.

It has been reported that all REE, except Ce, increase with depth in seawater to reach their maximum concentration near the bottom where Ce exhibit strong depletion which results in high anomalies [29]. Thus, the high REE concentrations and negative anomalies found in our sediment core could be partially attributed of the coastal upwelling activity affecting the northwest African coasts.

Conclusion

Levels of radionuclide concentrations in sediment from the bed channel in the Oualidia Lagoon did not show any enhancement, except for ^{210}Pb as a result of relatively high rate of delivery to the sediment despite the low mud content. Furthermore, the sediment core was dated using excess ^{210}Pb profile and applying a conventional model. Radionuclide activities versus grain size revealed markedly enriched fine particles but also relatively high radioactivity content in coarse particles. Some selected major elements and their ratios were used as proxies to establish the origin of sediment. Neither the seawater nor the terrigenous signals were found to be preserved in the bed sediment but a mixture of both, being in conformity with the location of the sampling site which is under the marine and continental influences. Elemental ratios and Cerium anomalies suggested two major input sources of REE to the bed sediment of the Oualidia Lagoon: (i) A contribution of terrigenous material. This component is likely to represent a small proportion of the REE budget in the sediment. (ii) Incorporation from seawater which is believed to be enriched with REE as a result of the prevailing coastal upwelling activity in the Atlantic Moroccan coast, and probably of anthropogenic activities in the surrounding studied area.

Acknowledgments This work has been carried out within the framework of the regional IAEA - TC project RAF/7/009 "Supporting an Integrated Approach for Marine Pollution Monitoring Using Nuclear Analytical Techniques", and the program REMER (*Réseau National des Sciences et Techniques de la Mer*) related to marine pollution.

References

1. Hilmi K, Koutitonsky VG, Orbi A, Lakhdar Idrissi J, Chagdali M (2005) Oualidia lagoon, Morocco: an estuary without a river. Afr J Aquat Sci 30(1):1–10
2. Hilmi K, Orbi A, Lakhdar Idrissi J (2009) Hydrodynamisme de la lagune de Oualidia (Maroc) durant l'été et l'automne 2005. Bull Inst Sci 31:29–34
3. Zourarah B, Maanan M, Carruesco C, Aajjane A, Mehdi K, Conceição Freitas M (2007) Fifty-year sedimentary record of heavy metal pollution in the lagoon of Oualidia (Moroccan Atlantic coast). Estuar Coast Shelf Sci 72:359–369
4. Maanan M, Ruiz-Fernández AC, Maanan M, Fattal P, Zourarah B, Sahabi M (2014) A long-term record of land use change impacts on sediments in Oualidia lagoon, Morocco. Int J Sediment Res 29:1–10
5. Rubio B, Nombela MA, Vilas F (2000) Geochemistry of major and trace elements in sediments of the Ria de Vigo (NW Spain): an assessment of metal pollution. Mar Pollut Bull 40:968–980
6. Lopez P, Navarro E, Marce R, Ordoñez J, Caputo L, Armengol J (2006) Elemental ratios in sediments as indicators of ecological processes in Spanish reservoirs. Limnetica 25(1–2):499–512
7. Tranchida G, Oliveri E, Angelone M, Bellanca A, Censi P, D'Elia M, Neri R, Placenti F, Sprovieri M, Mazzola S (2011) Distribution of rare earth elements in marine sediments from the Strait of Sicily (western Mediterranean Sea): evidence of phosphogypsum waste contamination. Mar Pollut Bull 62:182–191
8. Nie Y, Liu X, Emslie SD (2014) Distribution and sources of rare earth elements in ornithogenic sediments from the Ross Sea region, Antarctica. Microchem J 114:247–260
9. Laissaoui A, Benmansour M, Ziad N, IbnMajah M, Abril JM, Mulsow S (2008) Anthropogenic radionuclides in the water column and a sediment core from the Alboran Sea: application to radiometric dating and reconstruction of historical water column radionuclide concentration. J Paleolimnol 40(3):823–833
10. Kirchner G (2011) ^{210}Pb as a tool for establishing sediment chronologies: examples of potentials and limitations of conventional dating models. J Environ Radioact 102:490–494
11. Rharbi N, Ramdani M, Berrahou A, Lakhdar Idrissi A (2001) Caractéristiques hydrologiques et écologiques de la lagune de Oualidia, milieu paralique de la côte atlantique marocaine. Mar life 11(1–2):3–9
12. Matthews KM, Kim CK, Martin P (2007) Determination of ^{210}Po in environmental materials: a review of analytical methodology. Appl Radiat Isot 65:267–279

13. Brenner M, Claire L, Schelske CL, William FK (2004) Inputs of dissolved and particulate ^{226}Ra to lakes and implications for ^{210}Pb dating recent sediments. J Paleolimnol 32:53–66
14. Ramos-Lerate I, Barrera M, Ligero RA, Casas-Ruiz M (1998) A new method for gamma-efficiency calibration of voluminal samples in cylindrical geometry. J Environ Radioact 38(1):47–57
15. He Q, Walling DE (1996) Use of fallout ^{210}Pb measurements to investigate longer-term rates and patterns of overbank sediment deposition on the floodplains of lowland rivers. Earth Surf Process Landf 21:141–154
16. Kim Y, Kim K, Kang HD, Kim W, Doh SH, Kim DS, Kim BK (2007) The accumulation of radiocesium in coarse marine sediment: effects of mineralogy and organic matter. Mar Pollut Bull 54:1341–1350
17. United Nations Scientific Committee on Effects of Atomic Radiation (2000) Exposures from natural radiation sources, UNSCEAR Report, New York
18. Laissaoui A, Mas JL, Hurtado S, Ziad N, Villa M, Benmansour M (2013) Radionuclide activities and metal concentrations in sediments of the Sebou Estuary, NW Morocco, following a flooding event. Environ Monit Assess 185:5019–5029
19. Abril JM (2003) A new theoretical treatment of compaction and the advective-diffusive processes in sediments: a reviewed basis for radiometric dating models. J Paleolimnol 30(4):363–370
20. Freudenthal T, Meggers H, Henderiks J, Kuhlmann H, Moreno A, Wefer G (2002) Upwelling intensity and filament activity off Morocco during the last 250,000 years. Deep Sea Res Part II 49(17):3655–3674
21. Makaoui A, Orbi A, Hilmi S, Zizah K, Larissi J, Talbi M (2005) Upwelling of the Moroccan Atlantic coast between 1994 and 1998. C R Geosci 337(16):1518–1524
22. Ruiz-Fernandez AC, Hillaire-Marcel C, de Vernal A, Machain-Castillo ML, Vasquez L, Sholkovitz ER, Landing WM, Lewis BL (1994) Ocean particle chemistry: the fractionation of the rare earth elements between suspended particles and seawater. Geochim Cosmochim Acta 58:1567–1580
23. Taylor SR (1964) Trace element abundances and the chondritic Earth model. Geochim Cosmochim Acta 28(12):1989–1998
24. Bounouira H, Choukri A, Cherkaoui R, Gaudry A, Delmas R, Mariet C, Hakam OM, Chakiri S (2008) Multielement analytical procedure coupling INAA, ICP-MS and ICP-AES: application to the determination of major and trace elements in sediment samples of the Bouregreg river (Morocco). J Radioanal Nucl Chem 278(1):65–79
25. Lavilla I, Filgueiras AV, Valverde F, Millos J, Palanca A, Bendicho C (2006) Depth profile of trace elements in a sediment core of a high-altitude lake deposit at the Pyrenees, Spain. Water Air Soil Pollut 172(1–4):273–293
26. Taylor SR, McLennan SM (1985) The Continental Crust; its composition and evolution; an examination of the geochemical record preserved in sedimentary rocks. Blackwell, Oxford
27. Wei G, Liu Y, Li X, Shao L, Liang X (2003) Climatic impact on Al, K, Sc and Ti in marine sediments: evidence from ODP Site 1144, South China Sea. Geochem J 37:593–602
28. Gao S, Luo TC, Zhang BR, Zhang HF, Han YW, Zhao ZD, Hu YK (1998) Chemical composition of the continental crust as revealed by studies in East China. Geochim Cosmochim Acta 62:1959–1975
29. Zhang J, Nozaki Y (1996) Rare earth elements and yttrium in seawater: ICP-MS determinations in the East Caroline, Coral Sea, and South Fiji basins of the western South Pacific Ocean. Geochim Cosmochim Acta 60:4631–4644
30. De Baar HJW, Bacon MP, Brewer PG (1985) Rare earth elements in the Pacific and Atlantic oceans. Geochim Cosmochim Acta 49:1943–1959
31. Condie KC (1991) Another look at rare earth elements in shales. Geochim Cosmochim Acta 55:2527–2531
32. Oliveira SMB, Larizzatti FE, Fávaro DIT, Moreira SRD, Mazzilli BP, Piovano EL (2003) Rare earth element patterns in lake sediments as studied by neutron activation analysis. J Radioanal Nucl Chem 258(3):531–535
33. Kumar Krishnan, Saion Elias, Halimah MK, Yap CK, Hamzah Muhd Suhaimi (2014) Rare earth element (REE) in surface mangrove sediment by instrumental neutron activation analysis. J Radioanal Nucl Chem 301(3):667–676
34. Minai Y, Matsumoto R, Watanabe Y, Tominaga T (1992) Geochemistry of rare earths and other trace elements in sediments from sites 798 and 799, Japan Sea. In: Proceedings of the ocean drilling program, scientific results,s Vol 127/128
35. Nagarajan R, Madhavaraju J, Armstrong-Altrin JS, Nagendra R (2011) Geochemistry of neoproterozoic limestones of the Shahabad formation, Bhima basin, Karnataka, southern India. Geosci J 15(1):9–25